Bioresource Technology 343 (2022) 126063

Contents lists available at ScienceDirect

Bioresource Technology

journal homepage: www.elsevier.com/locate/biortech

Anaerobic co-digestion of various organic wastes: Kinetic modeling and synergistic impact evaluation

Renisha Karki [a,1], Wachiranon Chuenchart [b,1], K.C. Surendra [a,c], Shihwu Sung [d], Lutgarde Raskin [e], Samir Kumar Khanal [a,b,*]

[a] Department of Molecular Biosciences and Bioengineering, University of Hawai'i at Mānoa, 1955 East-West Road, Honolulu, HI 96822, USA
[b] Department of Civil and Environmental Engineering, University of Hawai'i at Mānoa, 2540 Dole Street, Honolulu, HI 96822, USA
[c] Global Institute for Interdisciplinary Studies, 44600 Kathmandu, Nepal
[d] College of Agriculture, Forestry and Natural Resource Management (CAFNRM), University of Hawai'i at Hilo, 200 W. Kawili Street, Hilo, HI 96720, USA
[e] Department of Civil and Environmental Engineering, University of Michigan, 1351 Beal Avenue, 107 EWRE Building, Ann Arbor, MI 48109-2125, USA

HIGHLIGHTS

- Coffee pulp and food waste mono-digestions yielded highest methane yields.
- Inoculum source had a significant effect on methane yields.
- No synergistic or antagonistic effect was observed for this study.
- Kinetic models were compared based on mono-digestion and co-digestion systems.
- Feedstock type had a major effect on the selection of the best-fit model.

ARTICLE INFO

Keywords:
Anaerobic co-digestion
Biochemical methane potential
Co-digestion performance index
Kinetic modeling
Synergistic effect

ABSTRACT

Anaerobic mono- and co-digestion of coffee pulp (CP), cattle manure (CM), food waste (FW) and dewatered sewage sludge (DSS), were assessed using biochemical methane potential tests. The effects of two different inocula, anaerobically digested cattle manure (ADCM) and anaerobically digested waste activated sludge (ADWAS), and five different co-feedstock ratios for CP:CM and FW:DSS (1:0, 4:1, 2:1, 4:3, and 0:1) on specific methane yields were also evaluated. Mono-digestions of both CP and FW yielded the highest methane yield compared to the co-digestion ratios examined. Furthermore, no synergistic or antagonistic effect was observed for any of the co-digestion ratios tested. Nine different kinetic models (five conventional mono-digestion models and four co-digestion models) were compared and evaluated for both mono- and co-digestion studies. For CP:CM, cone and modified Gompertz with second order equation models were the best-fit for mono- and co-digestion systems, respectively, while for FW:DSS, superimposed model showed the best-fit for all systems.

1. Introduction

"Closing the loop" approach in circular economy has been recognized as pivotal for energy security and the climate change mitigation (Bedoić et al., 2020). To strengthen this approach, a multi-waste management concept through anaerobic digestion (AD) has been implemented for decades. AD technology via anaerobic co-digestion has become widely popular in recent years to enhance methane and nutrient recovery, and to maintain overall digester stability (Mostafa Imeni et al., 2019). Co-digestion also has several advantages over mono-digestion in terms of improved methane yield and process stability due to synergistic interactions, nutrient balance, and dilution of toxic compounds (Karki et al., 2021). A wide array of feedstocks has been utilized for co-digestion including, but not limited to, sewage sludge, food waste (FW), agro-industrial wastes/residues, animal manure, and microalgae (Chuenchart et al., 2020; Dennehy et al., 2018; Paranhos et al., 2020; Zhen et al., 2016). However, the transport cost of the co-feedstocks from the generation point to the AD plant should be an important criteria

* Corresponding author.
E-mail address: khanal@hawaii.edu (S.K. Khanal).
[1] The authors contributed equally to this work.

https://doi.org/10.1016/j.biortech.2021.126063
Received 31 July 2021; Received in revised form 26 September 2021; Accepted 28 September 2021
Available online 5 October 2021

Table 1
Feedstocks and inocula characteristics (mean ± SD), n = 3.

Parameter	Unit	CP	CM	FW	DSS	ADCM	ADWAS
TS	%, wet basis	6.74 ± 0.07	15.36 ± 0.07	27.55 ± 0.08	8.68 ± 0.12	3.42 ± 0.01	3.08 ± 0.01
VS	%, TS	95.37 ± 0.07	82.84 ± 0.25	94.96 ± 0.11	80.49 ± 0.16	72.75 ± 0.09	64.24 ± 0.11
pH	N/A	3.74 ± 0.05	6.98 ± 0.05	4.10 ± 0.00	6.43 ± 0.02	8.06 ± 0.03	8.00 ± 0.05
TC	%, dry basis	44.90 ± 0.63	40.27 ± 0.25	51.88 ± 0.31	38.43 ± 0.05	n.a.	n.a.
TN	%, dry basis	1.64 ± 0.10	1.32 ± 0.11	3.09 ± 0.12	7.45 ± 0.03	n.a.	n.a.
C/N ratio	N/A	27.44 ± 1.81	30.66 ± 2.66	16.81 ± 0.56	5.16 ± 0.01	n.a.	n.a.
Cellulose	%, dry basis	29.63 ± 0.75	20.95 ± 0.73	n.a.	n.a.	n.a.	n.a.
Hemicellulose	%, dry basis	4.25 ± 0.77	18.29 ± 0.90	n.a.	n.a.	n.a.	n.a.
Lignin	%, dry basis	21.15 ± 0.74	15.17 ± 0.64	n.a.	n.a.	n.a.	n.a.

CP: Coffee pulp; CM: Cattle manure; FW: Food waste; DSS: Dewatered sewage sludge; ADCM: Anaerobically digested cattle manure; ADWAS: Anaerobically digested waste activated sludge; TS: Total solids; VS: Volatile solids; TC: Total carbon; TN: Total nitrogen; C/N ratio: Total carbon/Total nitrogen ratio; SD: Standard deviation; N/A: Not applicable; n.a.: Not analyzed.

while selecting co-feedstocks for co-digestion (Mata-Alvarez et al., 2014).

About 500 million US tons of agricultural wastes are produced annually in the U.S. (Kaza et al., 2018). Furthermore, approximately 900 million US tons/year of cattle manure (CM) are reported to be generated in the U.S. (Ma et al., 2020). Agricultural wastes and manures are the most convenient co-feedstocks during co-digestion which results in enhanced methane yields compared to mono-digestion (Ma et al., 2020; Mata-Alvarez et al., 2014). Globally, coffee has an annual production of about 10 million US tons (green coffee equivalents) (Londoño-Hernandez et al., 2020). Coffee pulp (CP) accounts for nearly 42% of the total wastes produced during coffee processing. AD has a potential for valorizing CP with bioenergy and organic fertilizer production. However, mono-digestion of CP poses several hurdles due to its low pH, elevated production of volatile fatty acids (VFA), and high levels of toxic compounds like caffeine, free phenols, and tannins (Rojas-Sossa et al., 2017). Hence, as a mitigation strategy, co-digestion of CP with CM could be a viable option (Selvankumar et al., 2017) due to dilution effect, microbial and nutrients supplementation, and high buffering capacity of CM.

In 2019, about 1 billion US tons of FW were generated which accounted for 17% of the total global food production (UNEP, 2021). In the U.S., there are 58 standalone AD plants that solely digest FW. Of the 1200 AD plants located at water resource recovery facilities (WRRFs) in the U.S., around 133 co-digest biosolids with various organic waste streams such as FW or high strength industrial byproducts (such as, glycerin). Such co-digestion plants reported to utilize an average of 0.1 million US tons of FW annually (Jones et al., 2019). Besides an advantage of utilizing excess capacity in existing digesters, co-digestion of FW with sewage sludge could result in improved methane yields and synergistic effect due to alkalinity supplementation and dilution of inhibitory compounds such as VFA (Karki et al., 2021; Pan et al., 2019).

Biochemical methane potential (BMP) test is a simple method to evaluate the biodegradability of feedstocks, thus facilitating in design of real AD plants and predicting optimal operating parameters (Holliger et al., 2016). Furthermore, the kinetic analysis of the BMP results provides information on the extent and rate of biodegradability of substrates. Kinetic models can reveal the bottlenecks that limit digestibility and methane yield (for instance, lag phase, substrate inhibition, etc.) (Tsapekos et al., 2018). Many studies adopted simplified conventional mathematical models (first order, second order, Chen and Hashimoto, modified Gompertz, transfer, and cone) to fit the experimental data of both mono- and co-digestion studies (Panigrahi et al., 2020). However, for mono-digestion of complex organic substrates or co-digestion, the best-fit models should consider the presence of a slow or non-biodegradable and readily biodegradable fractions. Thus, models may need to be modified to integrate more parameters (superimposed, modified Gompertz with second order, two-phase exponential, and multi-stage) that could more accurately predict the BMP, when components with different biodegradability patterns are present (Karki et al., 2021). To this end, the comprehensive kinetic study compares and evaluates both conventional kinetic models and co-digestion models to analyze the kinetics of methane production from the mono- and co-digestion of diverse organic wastes.

The objective of this study was to select optimal co-feedstock mixing ratio and inoculum source that maximizes the methane yield and to investigate the kinetics during mono-digestion and co-digestion of CP and CM, and FW and dewatered sewage sludge (DSS), at different mixing ratios. Moreover, there are only few studies that have analyzed CP as a feedstock for biomethane production as CP is known to contain many toxic components such as polyphenols, caffeine etc. (Corro et al., 2014; Selvankumar et al., 2017; Chala et al., 2019). Selection of a good source of inoculum, hence, is interesting to analyze during degradation of diverse inhibitory components in the feedstocks. Furthermore, nine different mathematical models were used for estimating the kinetic parameters of the tests, and for identifying the model that best describes the degradation kinetics of the studied feedstocks.

2. Materials and methods

2.1. Inocula and substrates collection and preparation

Fresh CM was collected from Kualoa ranch, Honolulu, HI, USA. CP waste was collected from Waialua Estate Coffee and Chocolate, Honolulu, HI, USA. CP waste was blended with water, in the ratio of 1:1 (w/w), using Vitamix (Vitamix VM0185A, USA). FW was collected for a week from University of Hawai'i at Mānoa cafeteria, homogenized and sub-sampled. After sub-sampling, the FW was blended with Vitamix (Vitamix VM0185A, USA). DSS (mixture of primary and secondary sludge retrieved from belt filter press) was obtained from Hawaii Kai wastewater treatment plant, Honolulu, HI, USA. All the feedstocks after

processing were stored in −20 °C freezer before use. Freezing is important to preserve the characteristics of feedstocks. Anaerobically digested cattle manure (ADCM) and anaerobically digested waste activated sludge (ADWAS) were used as inocula. ADCM was obtained from two mesophilic vertical anaerobic digesters maintained in lab for several years, which was fed with CM and supplied with micro-nutrients. ADWAS was collected from AD plant fed with DSS and operated under mesophilic condition in Hawaii Kai wastewater treatment plant, Honolulu, HI, USA. The inocula were stored at 4 °C in a walk-in refrigerator and used for BMP tests within a week. Astals et al. (2020) reported that the inoculum stored at 4 °C maintained methanogenic activity for up to 14 days before use. The characteristics of feedstocks and inocula are summarized in Table 1. The analyses were performed in triplicates.

2.2. Biochemical methane potential (BMP) test

Batch tests were carried out to assess the maximal methane production potential of co-feedstocks at five different mixing ratios (1:0, 4:1, 2:1, 4:3, 0:1) based on volatile solids (VS). Two sets of batch AD experiments were conducted at mesophilic conditions. The first set of experiments utilized CP and CM while the second set contained FW and DSS. Each set was subdivided into two sub-sets based on the inoculum used (ADCM or ADWAS). BMP test was conducted using a series of 250-mL serum bottles with the working volume of 180 mL and the inoculum to substrate ratio (ISR) of 1.0 (VS basis). The total substrate (VS) concentration fed to each serum bottle was adjusted at 1.5% by adding water. The serum bottles were then sealed with a screw cap and a rubber septum. The headspace was flushed with N_2 gas, as recommended by Holliger et al. (2016) for small head-space volume reactors, and the bottles were continuously agitated at 120 rpm at 37 ± 1 °C. The biogas was collected in 0.5 L Tedlar bags connected to the serum bottles. BMP test was terminated after 50 days when the daily biogas production was <1% of the total biogas production. Blank assays containing only inoculum were used to correct for the background methane potential of the inoculum. All the experiments were performed in triplicate.

2.3. Analytical methods

TS and VS of feedstocks were determined as per Standard Methods (APHA, 2017). The total carbon and total nitrogen of feedstocks were analyzed via high temperature combustion interfaced to an isotope ratio mass spectrometry (IRMS) (Costech, Elemental Analyzer, USA). pH was measured using titrator (Hach, TitraLab AT1000, USA) with pH probe (PHC805). Fiber compositions (neutral detergent fiber (NDF), acid detergent fiber (ADF), and acid detergent lignin (ADL)) of the feedstocks were analyzed following the AOAC (2006) methods. The cellulose and hemicellulose contents were calculated using equations: cellulose = ADF – ADL, and hemicellulose = NDF – ADF. The volume of the daily biogas production was quantified using Ritter Drum Type Gas Meter (Ritter, TG 0.5/5, Germany), while biogas composition was analyzed using gas chromatography equipped with thermal conductivity detector (GC-TCD) (Agilent, 490 Micro GC System, USA). Biogas volumes were normalized to standard temperature (273 K) and pressure (1 atm) and reported as N mL.

2.4. Co-digestion performance index calculation

The co-digestion performance index (CPI) or synergistic index was calculated to evaluate the synergistic effect of co-digestion for varying feedstock mixing ratios. The index was determined as the ratio of observed to expected methane yields. The expected methane yield of a mixture was estimated as the weighted average of methane yields from mono-digestion of individual feedstocks. CPI values depict the possible interactions in co-digestion processes; antagonistic (CPI < 1), additive (CPI = 1), and synergistic (CPI > 1) (Ebner et al., 2016).

2.5. Kinetic models

In this study, nine kinetic models were selected to fit the methane production data from the selected organic wastes. The kinetic analysis helps to elucidate the best-fit model based on the fitting of model-predicted values with BMP experimental values. The models in this study were adapted to evaluate methane production instead of biogas production.

2.5.1. First order kinetic model

This is the most widely used model when hydrolysis is the rate-limiting step in AD process, for example when lignocellulosic feedstock is used as a substrate.

$$G = G_0 \cdot [1 - e(-kt)] \quad (1)$$

where, G: Cumulative methane yield at digestion time t (mL/g VS_{added}); G_0: Specific methane yield of substrates (mL/g VS_{added}); k: Methane production rate constant (first order disintegration rate constant) (1/day); t: Time (days).

In this case, k describes the rates of degradation and methane production; hence, high k corresponds to high rates of degradation and methane production (Mao et al., 2017).

2.5.2. Modified Gompertz model

This model is used when inhibition is observed in the AD process assuming methane production reflects bacterial growth (Mao et al., 2019). The modified Gompertz model is given by:

$$G = G_0 \cdot e\left\{ -e\left[\frac{R_m \cdot e}{G_0}(\lambda - t) + 1\right]\right\} \quad (2)$$

where, G: Cumulative methane yield (mL/g VS_{added}) over time t; G_0: Specific methane yield of substrates (mL/g VS_{added}); R_m: Maximum methane production rate (mL/g VS_{added}/day); λ: Lag phase (days); t: Time (days).

2.5.3. Chen and Hashimoto model

This model is considered reliable when used for the predictions of AD of feedstocks with substantial amount of total solids content (Kafle and Chen, 2016).

$$G = G_0 \cdot \left[1 - \frac{k_{CH}}{(HRT \cdot \mu_m) + k_{CH} - 1}\right] \quad (3)$$

G: Cumulative methane yield at digestion time t (mL/g VS_{added}); G_0: Specific methane yield of substrates (mL/g VS_{added}); k_{CH}: Chen and Hashimoto constant (dimensionless); μ_m: Maximum specific growth rate

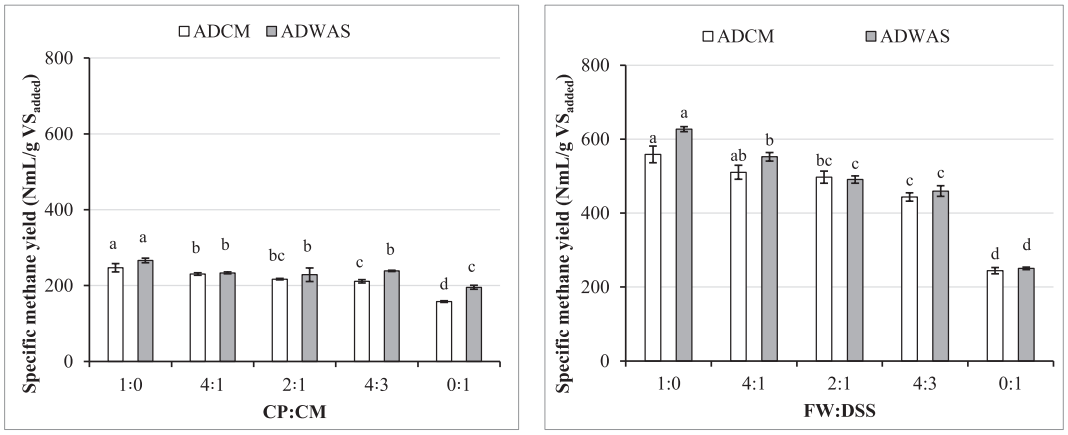

Fig. 1. Specific methane yields for co-digestion of (a) CP and CM and (b) FW and DSS. CP: Coffee pulp; CM: Cattle manure; FW: Food waste; DSS: Dewatered sewage sludge; ADCM: Anaerobically digested cattle manure; ADWAS: Anaerobically digested waste activated sludge. The co-digestion mixing ratios mentioned in the figure are based on volatile solids (VS). The letters denote statistical significance at $p < 0.05$.

of microorganisms (1/day); HRT: Digestion time or hydraulic retention time (days).

2.5.4. Transfer model

Transfer model is derived from the first order kinetic model where the kinetic constant is substituted for the ratio of maximum methane production rate to methane potential of substrate (Zahan et al., 2018).

$$G = G_0 \cdot \left\{ 1 - e\left[\frac{-R_m}{G_0}(t-\lambda) \right] \right\} \quad (4)$$

In this model, G: Cumulative methane yield (mL/g VS_{added}); G_0: Specific methane yield of substrates (mL/g VS_{added}); R_m: Maximum methane production rate (mL/g VS_{added}/day); λ: Lag phase (days); t: Time (days).

2.5.5. Cone model

Cone model is an empirical model that was developed to evaluate the methane production from specific substrate in the presence of ruminal microorganism (Lima et al., 2018). The cone model allows the determination of specific methane production rate and maximum cumulative methane production. Furthermore, this model estimates the behavior of methane production by the shape factor (n), which indicates the presence or absence of lag phase.

$$G = \frac{G_0}{1 + (kt)^{-n}} \quad (5)$$

where, G: Cumulative methane yield (mL/g VS_{added}); G_0: Specific methane yield of substrates (mL/g VS_{added}); k: Cone kinetic constant (1/day); n: Shape factor (dimensionless) [value that is affected by an object's shape but is independent of its dimensions]; t: Time (days).

2.5.6. Superimposed model

Superimposed model was developed by coupling the first order kinetic model with modified Gompertz model and assumes that during the digestion of certain feedstocks, two peaks exist. The first peak is related to rapid utilization of easily biodegradable substrates, while the second peak corresponds to the poorly degradable substrates (Wang et al., 2020b).

$$G = G_{01}[1 - e(-k \cdot t)] + G_{02} \cdot e\left\{ -e\left[\frac{R_m \cdot e}{G_{02}} \cdot (\lambda - t) + 1 \right] \right\} \quad (6)$$

where, G_{01}: Maximum specific methane yield from the easily biodegradable substrates (mL/g VS_{added}); G_{02}: Maximum specific methane yield from the poorly biodegradable substrates (mL/g VS_{added}); k: Biogas or methane production rate constant (first order disintegration rate constant) (1/day); R_m: Maximum methane production rate (mL/g VS_{added}/day); λ: Lag phase (days); t: Time (days).

2.5.7. Modified Gompertz with second order equation

This model was developed by coupling the second order kinetic model with modified Gompertz model. The Gompertz model was modified to fit the methane production dynamics in anaerobic co-digestion processes, which typically show two stages of methane production (Masih-Das and Tao, 2018).

$$G = G_{01}\left[\frac{t}{k+t} \right] + G_{02} \cdot e\left\{ -e\left[\frac{R_m \cdot e}{G_{02}} \cdot (\lambda - t) + 1 \right] \right\} \quad (7)$$

where, G: Specific methane yield at t (mL/g VS); G_{01} and G_{02}: Specific methane yields at the first and second stages (mL/g VS); R_m: Maximum specific methane production rate (mL/g VS/day); k: First-stage half saturation time (days); λ: Lag phase (days), t: Time (days).

2.5.8. Two-phase exponential model

The two-phase exponential model describes the behavior of biogas production in two or more stages. The two-phase model evaluates the substrate conversion to biogas for each phase (Lima et al., 2018).

$$G = G_{01}[1 - e(-k_1 \cdot t)] + G_{02}[1 - e(-k_2 \cdot t)] \quad (8)$$

where, G_{01}: Specific methane yield in first phase (mL/g VS); G_{02}: Specific methane yield in second phase (mL/g VS); k_1: Kinetic rate constant for first phase (1/day); k_2: Kinetic rate constant for second phase (1/day); t: Time (days).

2.5.9. Multi-stage model

Unlike two-phase model, multi-stage model considers the interactions between each stage for the total biogas production. This model depicts the behavior of biogas production based on different substrates, stages, and their interactions (Lima et al., 2018).

$$P = A_S[1 - e(-k_1 \cdot t)] + A_I[1 - e(-k_2 \cdot t)] + A_{IS}\left[1 - \frac{k_2 \cdot e(-k_1 \cdot t)}{k_2 - k_1} - \frac{k_1 \cdot e(-k_2 \cdot t)}{k_1 - k_2}\right] \quad (9)$$

where, A_S, A_I, A_{IS}: Accumulated specific methane yield in each stage (mL/g VS); k_1 and k_2: Kinetic rate constants in each stage (1/day); t: Time (days).

The unknown parameters for all the above-mentioned models were estimated by non-linear regression using the Solver tool of the Microsoft Excel program. The values were selected based on the least sum of the squares of the differences between predicted and experimental values of cumulative specific methane production.

2.5.10. Models evaluation

The goodness of fit and capability of the kinetic models to describe the biodegradability process was evaluated using the coefficient of determination (R^2), adjusted R^2 (R^2 Adj), root mean square error (RMSE), and Akaike's information criterion (AIC).

2.6. Statistical analysis

The specific methane yields were analyzed using factorial design in R statistical package (RStudio, R studio v.1.2.5033, USA). Two-way analysis of variance (ANOVA) followed by the Tukey's honestly significant difference (HSD) for multiple comparison test ($p < 0.05$) were conducted.

3. Results and discussion

3.1. Biomethane generation potential of various organic wastes

Significant difference was observed between different mixing ratios of CP and CM and different inocula ($p < 0.01$) (Fig. 1). For both inocula, mono-digestion of CP and CM resulted in the highest and the lowest specific methane yield (SMY), respectively. The observed methane yield for CP was in accordance with literature values (Chala et al., 2019). Similarly, the methane yield for CM was in line with a study based on a meta-analysis of methane yields from CM mono-digestion during batch test (Ma et al., 2020). However, there was no significant difference between SMYs of mixing ratios of CP:CM 4:1, 2:1, and 4:3 for ADWAS inoculum. For ADCM inoculum, the increase in SMY was directly proportional to the increase in the proportion of CP in the mixture.

Similarly for FW and DSS, ADWAS resulted in significantly higher SMY than ADCM ($p < 0.001$), which could be because of better adaptability of ADWAS inoculum to degrade diverse organic wastes. The SMYs of different mixing ratios were significantly different ($p < 0.001$). Higher FW to DSS ratio resulted in higher SMY due to the abundance of readily biodegradable components in FW. The SMYs of FW mono-digestion (558.63 and 626.82 mL/g VS_{added} for ADCM and ADWAS, respectively) are in the range of SMYs for FW as mentioned in Karki et al. (2021). These higher SMYs might be due to higher lipid content in FW (Elalami et al., 2019). FW mono-digestion (FW:DSS ratio of 1:0) with ADWAS yielded the highest methane yield. The significant percent increase in SMY, 82% for ADCM and 84% for ADWAS, was observed for FW:DSS ratio of 4:1 compared to mono-digestion of DSS. For ADCM, there was no significant difference for co-feedstock ratios of 1:0 and 4:1, and 2:1 and 4:3. For ADWAS, no significant difference was observed for FW:DSS ratios of 2:1 and 4:3.

In all the BMP tests regardless of feedstocks used, ADWAS inoculum showed higher SMYs ($p < 0.05$) compared to ADCM which could be because of better adaptability of ADWAS to different substrates compared to ADCM (Lima et al., 2018). Furthermore, the CPI values showed additive interaction (0.9–1.1) for the co-digestion of all feedstocks. Especially for FW:DSS, similar additive effect was reported in other studies (Koch et al., 2015; Liu et al., 2016; Gu et al., 2020). Two inferences can be drawn from the CPI results; a) Higher methane yield does not necessarily guarantee the enhancement of synergistic effect of co-digestion (Karki et al., 2021), and b) CP:CM and FW:DSS can be co-digested without antagonistic effect at any feedstocks mixing ratio > 50% (VS basis) based on the co-feedstock ratios studied. However, it should be noted that BMP tests should not be considered to analyze any synergistic or antagonistic effect and the BMP of co-digestion should be close to weighted average of individual substrates (Koch et al., 2020).

3.2. Evaluation of the tested kinetic models

Kinetic models can identify the bottlenecks that limit methane production (for instance, lag phase) and identify SMY of co-digestion, acute toxicity, and kinetic parameters for the process optimization (Tsapekos et al., 2018; Koch et al., 2020). Data modeling for the feedstocks depicts the kinetic parameters estimated by fitting the modified Gompertz, Chen and Hashimoto, first order, transfer, cone, superimposed, modified Gompertz with second order equation, two-phase exponential, and multi-stage models to the experimental data obtained from the BMP tests. As summarized in Table 2, the kinetic models were validated based on the values of error functions (R^2 Adj, RMSE, and AIC) that minimize the differences between experimental and predicted data (Lima et al., 2018).

For the first set of BMP tests (CP:CM), all models resulted in an R^2 Adj higher than 0.95, indicating the best-fit of the model to the experimental data. However, R^2 Adj alone should not be used to validate the suitability of the model, and the combination of R^2 Adj, RMSE, and AIC values, and expected unknown parameters should be considered. While R^2 Adj and AIC might be useful for models' comparison, R^2 and RMSE could be used as overall comparison. Comparing the quality of fits provided by all the kinetic models evaluated using R^2 Adj and RMSE values, it was observed that, on average, the modified Gompertz with second order equation model followed by cone and superimposed models best-fitted the experimental data for methane production. Furthermore, for ADCM, cone model was the best fit for the predicted SMY values, while modified Gompertz with second order equation model was the best fit for ADWAS inoculum. Modified Gompertz with second order equation assumes that methane production occurs in two

Table 2
Summary results of kinetic analysis using different models for co-digestion of coffee pulp (CP) and cattle manure (CM) at different mixing ratios by volatile solids (VS).

CP:CM Parameter	Unit	ADCM					ADWAS				
		1:0	4:1	2:1	4:3	0:1	1:0	4:1	2:1	4:3	0:1
Experimental values											
B_0	mL/g VS_{added}	381.58	342.86	328.85	302.63	204.09	448.80	377.28	366.86	368.92	274.13
	S.D.	15.93	5.22	1.24	7.78	2.73	4.34	5.10	27.02	7.56	5.55
G_0	mL/g VS_{added}	246.98	230.37	216.96	211.24	157.83	266.13	233.46	228.55	238.80	195.38
	S.D.	10.82	3.44	1.77	4.60	2.28	6.22	2.34	17.92	1.62	5.34
First order model											
G_0	mL/g VS_{added}	256.89	253.66	223.94	216.25	162.80	258.37	223.17	221.90	229.90	248.11
	% difference	4.01	3.35	3.22	2.37	3.15	3.00	4.61	3.00	3.87	26.99
k	1/day	0.09	0.10	0.10	0.10	0.07	0.27	0.22	0.19	0.15	0.03
R^2	N/A	0.9888	0.9862	0.9895	0.9908	0.9908	0.9747	0.9679	0.9934	0.9832	0.9721
R^2 Adj	N/A	0.9850	0.9807	0.9860	0.9871	0.9872	0.9675	0.9588	0.9901	0.9776	0.9582
RMSE	N/A	11.77	13.35	10.34	9.79	6.88	15.38	14.54	7.13	11.08	13.26
AIC	N/A	50.38	47.87	48.05	42.91	37.26	60.37	59.25	34.49	49.30	43.19
Modified Gompertz model											
G_0	mL/g VS_{added}	243.37	241.35	208.59	204.58	146.91	248.00	205.74	208.39	204.49	191.91
	% difference	1.48	1.69	4.01	3.25	7.43	7.31	13.48	9.67	16.78	1.81
R_m	mL/g VS_{added}/day	21.85	21.98	23.00	20.76	14.33	69.77	61.92	45.61	51.15	11.32
λ	days	1.35	1.54	1.75	1.47	2.41	0.68	0.82	0.40	0.79	5.17
R^2	N/A	0.9949	0.9980	0.9910	0.9934	0.9729	0.9831	0.9430	0.9459	0.8978	0.9986
R^2 Adj	N/A	0.9918	0.9965	0.9855	0.9885	0.9526	0.9746	0.9145	0.8918	0.8364	0.9972
RMSE	N/A	6.97	4.57	8.24	6.91	10.15	12.14	19.25	20.06	26.78	3.06
AIC	N/A	45.76	36.30	48.76	42.94	49.08	59.93	69.15	55.98	69.98	29.65
Chen and Hashimoto model											
G_0	mL/g VS_{added}	316.33	309.33	273.73	260.28	204.51	290.47	253.42	251.98	266.05	365.82
	% difference	28.08	26.04	26.16	23.22	29.58	9.15	8.55	10.26	11.41	87.23
k_{CH}	N/A	19.15	18.59	17.27	17.51	21.14	18.06	20.70	150.15	86.38	51.60
μ_m	1/day	1.87	1.96	1.80	2.05	1.64	6.22	5.84	34.52	16.07	1.36
R^2	N/A	0.9779	0.9744	0.9792	0.9811	0.9882	0.9635	0.9723	0.9978	0.9933	0.9681
R^2 Adj	N/A	14.28	15.82	12.16	11.61	6.65	17.80	13.40	4.20	6.83	13.65
RMSE	N/A	316.33	309.33	273.73	260.28	204.51	290.47	253.42	251.98	266.05	365.82
AIC	N/A	65.85	65.51	62.97	60.57	51.64	73.59	67.91	48.10	52.57	64.59
Transfer model											
G_0	mL/g VS_{added}	261.78	260.16	222.67	220.31	158.08	259.01	217.55	219.62	217.60	214.86
	% difference	5.99	6.00	2.63	4.30	0.16	2.75	7.32	4.06	9.74	9.97
R_m	mL/g VS_{added}/day	21.85	21.98	23.00	20.76	14.33	69.77	61.92	45.61	51.15	11.32
λ	days	0.22	0.20	0.51	0.24	0.70	0.12	0.26	0.03	0.24	1.28
R^2	N/A	0.9849	0.9797	0.9913	0.9866	0.9915	0.9747	0.9630	0.9914	0.9586	0.9653
R^2 Adj	N/A	0.9759	0.9645	0.9861	0.9766	0.9851	0.9621	0.9445	0.9828	0.9338	0.9305
RMSE	N/A	11.98	14.34	7.86	9.96	5.67	14.83	15.56	8.02	17.13	14.43
AIC	N/A	55.50	54.61	47.92	48.77	39.75	63.94	64.89	43.14	61.93	51.37
Cone model											
G_0	mL/g VS_{added}	258.73	250.72	223.97	216.88	166.82	256.54	229.63	242.64	264.71	200.99
	% difference	4.76	2.16	3.23	2.67	5.70	3.74	1.67	6.17	10.85	2.87
k	1/day	0.14	0.14	0.15	0.15	0.11	0.40	0.33	0.25	0.19	0.07
n	N/A	1.79	2.14	1.84	1.87	1.61	2.05	1.49	1.12	1.02	2.71
R^2	N/A	0.9972	0.9984	0.9997	0.9997	0.9961	0.9923	0.9811	0.9985	0.9932	0.9995
R^2 Adj	N/A	0.9955	0.9972	0.9996	0.9994	0.9932	0.9884	0.9717	0.9970	0.9891	0.9990
RMSE	N/A	5.13	4.30	1.38	1.53	3.97	8.24	11.22	3.33	6.91	1.99
AIC	N/A	40.23	35.35	16.62	18.80	34.05	52.19	58.35	30.86	45.59	23.62
Superimposed model											
G_{01}	mL/g VS_{added}	107.08	123.82	110.25	138.27	88.95	131.09	118.17	113.19	119.19	134.60
G_{02}	mL/g VS_{added}	141.41	123.82	110.25	78.27	88.95	131.30	118.41	113.19	119.19	134.60
	% difference	0.61	0.90	1.63	2.51	12.72	1.43	1.34	0.96	0.18	37.78
R_m	mL/g VS_{added}/day	0.12	0.23	0.21	0.14	0.08	0.84	0.59	0.01	0.02	0.10
k	1/day	0.10	0.07	0.06	0.07	0.05	0.08	0.07	0.28	0.27	0.03
λ	days	1.95	2.31	1.48	2.23	2.71	0.80	0.98	7.17	9.57	6.65
R^2	N/A	0.9978	0.9999	0.9994	0.9989	0.9946	0.9980	0.9985	0.9963	0.9929	0.9995
R^2Adj	N/A	0.9942	0.9996	0.9984	0.9962	0.9811	0.9954	0.9965	0.9777	0.9811	0.9970
RMSE	N/A	4.57	0.99	2.18	2.94	4.68	4.27	3.18	5.62	7.37	1.86
AIC	N/A	57.35	39.88	44.04	57.25	64.69	54.01	48.12	94.16	65.95	78.72
Modified Gompertz with second order equation model											
G_{01}	mL/g VS	91.26	129.45	108.79	117.06	167.67	130.83	154.75	227.92	228.15	129.47
G_{02}	mL/g VS	172.65	141.47	137.01	130.22	64.54	151.82	108.21	24.69	51.06	128.24
	% difference	6.85	10.39	13.29	17.07	47.13	6.21	12.63	10.53	16.92	31.90
R_m	mL/g VS/day	15.85	20.66	15.63	17.29	9.83	67.44	66.25	30.82	39.20	9.39
k	days	10.14	11.01	16.26	19.53	36.93	6.66	10.23	5.22	9.35	45.60
λ	days	1.77	3.51	1.73	1.84	2.31	1.01	1.16	1.34	0.92	6.57
R^2	N/A	0.9976	0.9997	0.9991	0.9988	0.9953	0.9994	0.9981	0.9996	0.9985	0.9997
R^2 Adj	N/A	0.9936	0.9991	0.9977	0.9957	0.9836	0.9987	0.9957	0.9978	0.9959	0.9981
RMSE	N/A	4.81	1.59	2.56	3.02	4.35	2.25	3.54	1.66	3.26	1.42
AIC	N/A	58.28	47.44	46.91	57.68	63.51	41.22	50.30	77.14	51.27	74.90
Two-phase exponential model											
G_{01}	mL/g VS	23.85	43.29	34.72	75.97	25.14	118.07	70.29	113.89	148.63	35.18

(*continued on next page*)

Table 2 (*continued*)

CP:CM Parameter	Unit	ADCM					ADWAS				
		1:0	4:1	2:1	4:3	0:1	1:0	4:1	2:1	4:3	0:1
G_{02}	mL/g VS	233.04	210.37	189.22	140.29	137.66	243.66	174.99	116.70	96.27	212.93
	% difference	4.01	3.35	3.21	2.38	3.15	35.92	5.06	0.89	2.55	26.99
k_1	1/day	0.09	0.10	0.10	0.10	0.08	0.01	0.04	0.08	0.07	0.03
k_2	1/day	0.09	0.10	0.10	0.10	0.08	0.29	0.29	0.35	0.40	0.03
R^2	N/A	0.9888	0.9862	0.9895	0.9908	0.9908	0.9769	0.9764	0.9983	0.9942	0.9721
R^2 Adj	N/A	0.9776	0.9678	0.9790	0.9785	0.9786	0.9585	0.9576	0.9950	0.9884	0.9163
RMSE	N/A	11.77	13.35	10.34	9.79	6.88	14.89	12.83	3.56	6.46	13.27
AIC	N/A	62.38	62.80	60.05	57.84	52.20	70.01	67.04	45.79	51.58	64.19
Multi-stage model											
A_S	mL/g VS	0.02	1.97	1.00	4×10^{-5}	3×10^{-3}	4.5×10^{-5}	2.32	2.33	2.34	4×10^{-4}
A_I	mL/g VS	34.47	1.97	0.84	2×10^{-4}	4×10^{-5}	2×10^{-4}	183.72	142.87	122.21	3×10^{-4}
A_{IS}	mL/g VS	212.17	240.13	214.43	210.61	157.71	252.67	59.24	85.39	120.36	202.70
	% difference	0.13	0.55	0.32	0.30	0.08	5.33	5.06	0.89	2.55	3.74
k_1	1/day	0.22	0.27	0.15	0.15	0.10	1.29	0.04	0.08	0.07	0.11
k_2	1/day	0.21	0.21	0.54	0.63	0.79	0.42	0.31	0.31	0.40	0.11
R^2	N/A	0.9986	0.9984	0.9998	0.9992	0.9961	0.9857	0.9764	0.9983	0.9942	0.9934
R^2 Adj	N/A	0.9962	0.9943	0.9994	0.9973	0.9864	0.9678	0.9470	0.9900	0.9846	0.9606
RMSE	N/A	3.62	4.00	1.33	2.43	3.95	11.28	12.83	3.56	6.46	6.24
AIC	N/A	53.16	62.18	35.00	54.24	61.99	73.45	76.04	87.79	63.58	95.63

The table summarizes the results of kinetic analyses at different mixing ratios (1:0. 4:1, 2:1, 4:3, and 0:1) and different inocula for mono-digestion and co-digestion of coffee pulp (CP) and cattle manure (CM). ADCM: Anaerobically digested cattle manure; ADWAS: Anaerobically digested waste activated sludge; B_0: Maximum specific biogas yield of substrates; G_0, G_{01}, G_{02}, A_S, A_I, A_{IS}: Maximum specific methane yield of substrates at respective phase and stage; R_m: Maximum methane production rate; λ: Lag phase, t: Time (days); k_{CH}: Chen and Hashimoto constant; μ_m: Maximum specific growth rate of microorganisms; k (1/day): Methane production rate constant (first order disintegration rate constant); k: Cone kinetic constant; n: Shape factor; k (days): First-stage half saturation time; k_1 and k_2: kinetic rate constants; R^2: Coefficient of determination; R^2 Adj: Adjusted R^2; RMSE: Root mean square error; AIC: Akaike's information criterion, N/A: Not applicable.

stages, readily degradable and recalcitrant components of the feedstocks (Masih-Das and Tao, 2018).

Furthermore, AIC values did not correspond well with the R^2 Adj and RMSE values. Based on AIC values, cone model best-fitted the experimental data on average (34.45), for ADCM (29.01) and ADWAS (41.25) inocula. This could be because AIC is biased towards the number of parameters in the model and thus, favors the model with lower number of independent variables with a good fit compared to complex models.

The methane production potential is one of the parameters for validating the model. Among the nine models used, the multi-stage kinetic model showed the least difference (0.1–5.3%) between the experimental and predicted SMY followed by cone model (1.7–10.9%). On the other hand, Chen and Hashimoto model depicted the highest difference (8.6–87.2%).

Lag phase time (λ) depicts microbial adaptation to the substrates. In all the models predicting lag phase, lag periods of mono- and co-digestions of CP and CM were shorter in ADWAS compared to ADCM inoculum, except in the case of mono-digestion of CM. This could be because ADWAS as an inoculum provides diverse consortia of microorganisms to degrade the potential toxic components of CP. In contrast, lag period of mono-digestion of CM in ADCM inoculum was shorter than that in ADWAS inoculum possibly because the microorganisms in ADCM inoculum could be more acclimatized to degrade CM. Furthermore, the value of cone constant ($n > 1$) indicates the presence of lag phase. The mono-digestion systems had higher n values in ADWAS compared to ADCM while the co-digestion systems had lower n values in ADWAS compared to ADCM inoculum. This value was in conjunction with modified Gompertz and modified Gompertz with second order equation models (Fig. 2).

For the second set of BMP tests (FW:DSS), all models resulted in R^2 Adj > 0.89 as depicted in Fig. 3 and Table 3. Co-digestion models fit the results better compared to mono-digestion models based on R^2 Adj, and RMSE (Table 3). The co-digestion models also fit better with mono-digestion results.

Among conventional mono-digestion models based on R^2 Adj and RMSE, the cone model (0.9929 and 11.27) showed the highest accuracy, followed by the modified Gompertz (0.9618 and 21.37), and transfer (0.9616 and 27.58) models. For co-digestion models, superimposed model (0.9954 and 6.71) followed by modified Gompertz with second order model (0.9949 and 7.27) and multi-stage model (0.9859 and 12.38) showed the best fit. For both inocula, superimposed followed by modified Gompertz with second order and cone models depicted the best fit. For ADCM, R^2 Adj of superimposed, modified Gompertz with second order and cone models were 0.9936, 0.9929, and 0.9923 with RMSE of 7.53, 8.35, and 10.44, respectively. For the same models with ADWAS, R^2 Adj of 0.9973, 0.9970, and 0.9934 with respective RMSE values of 5.90, 6.19, and 12.09 were observed.

Both superimposed and modified Gompertz with second order models, which describe the readily and slowly biodegradable fractions of feedstocks, are based on modified Gompertz model (Masih-Das and Tao, 2018; Wang et al., 2020b). The only difference is that for the rapidly biodegradable components, the superimposed model relies on the first-order model. Compared with CP and CM, FW and DSS have lower substrate complexity, so the models showed only two stages instead of fitting with the multi-stage model.

The average AIC values of 56.52–59.30 for the three best-fit models suggest lower prediction errors compared with others (68.13–78.06). The average percent difference of SMYs between observed and predicted values were lower than 10% for all models except modified Gompertz model with second order for ADCM (25.67%) and Chen and Hashimoto model for both ADCM and ADWAS (33.12 and 28.65%, respectively).

The kinetic constants (1/day) of the first-order model were higher for

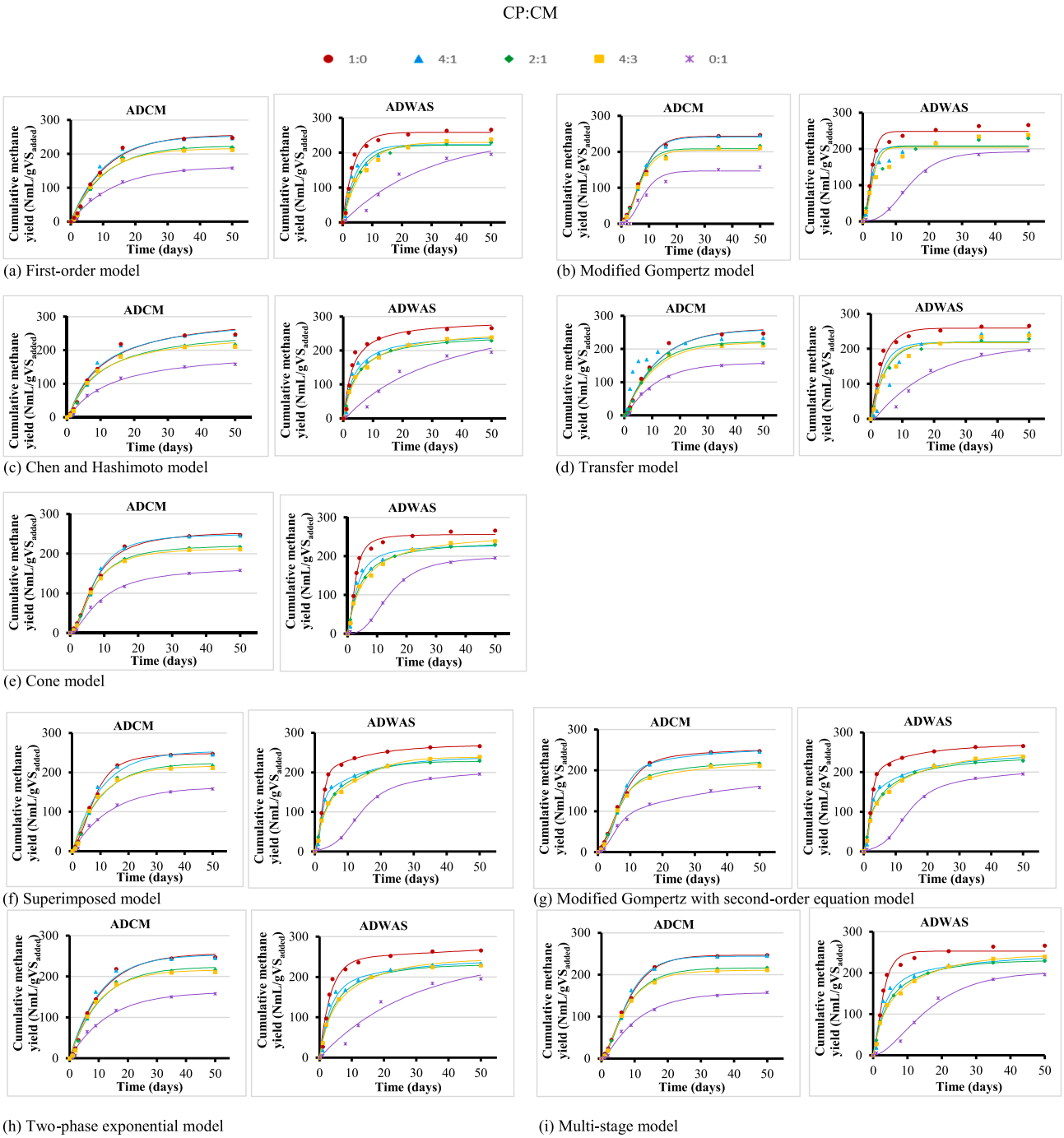

Fig. 2. Fitting BMP data of co-digestion of coffee pulp and cattle manure (CP:CM) to kinetic models. ADCM: Anaerobically digested cattle manure; ADWAS: Anaerobically digested waste activated sludge. The markers indicate BMP experimental data and lines indicate model prediction.

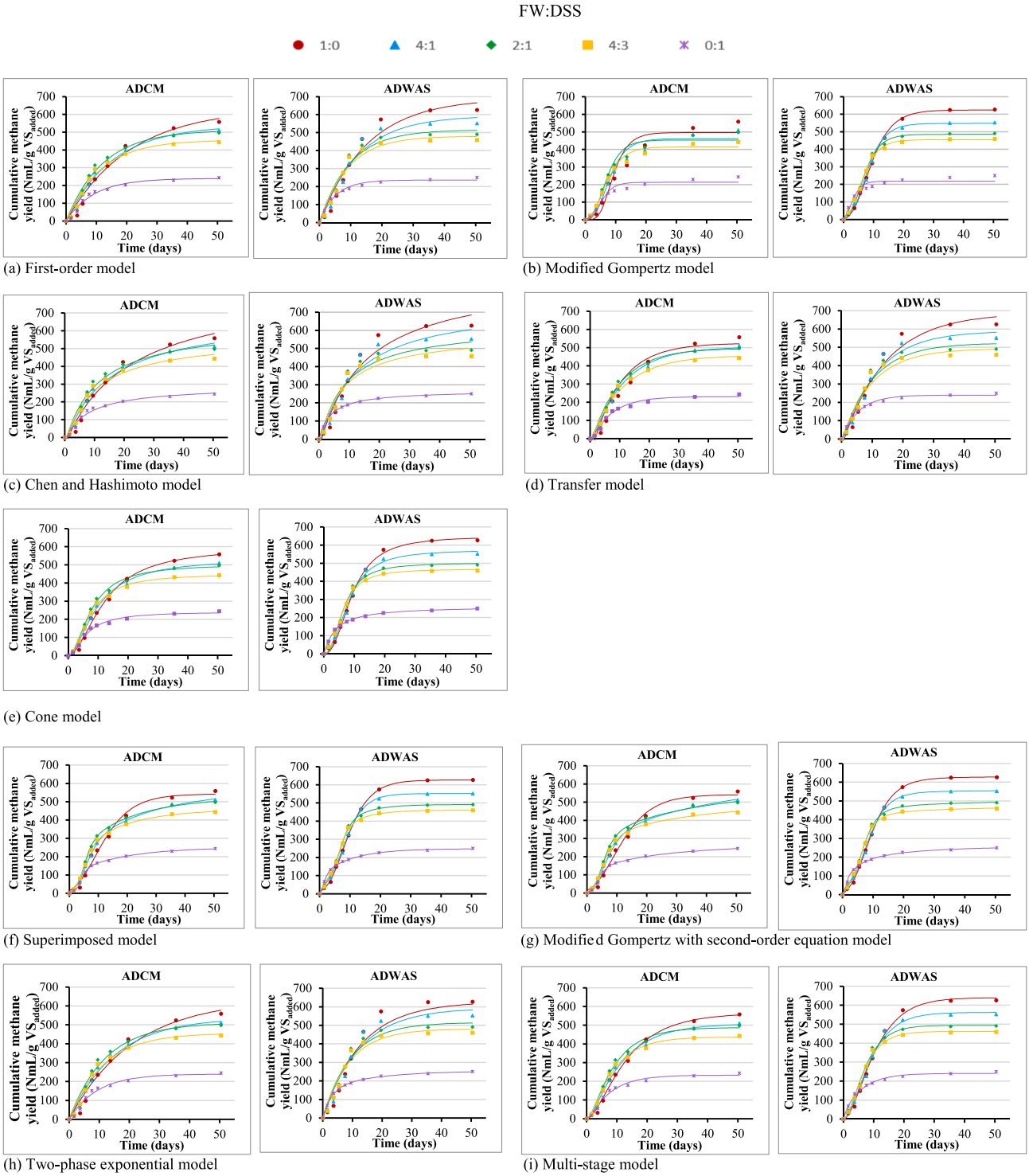

Fig. 3. Fitting BMP data of co-digestion of food waste and dewatered sewage sludge (FW:DSS) to kinetic models. ADCM: Anaerobically digested cattle manure; ADWAS: Anaerobically digested waste activated sludge. The markers indicate BMP experimental data and lines indicate model prediction.

Table 3
Summary results of kinetic analysis using different models for co-digestion of food waste (FW) and dewatered sewage sludge (DSS) at different mixing ratios by volatile solids (VS).

FW:DSS Parameter	Unit	ADCM					ADWAS				
		1:0	4:1	2:1	4:3	0:1	1:0	4:1	2:1	4:3	0:1
Experimental values											
B_0	mL/g VS_{added}	795.04	707.11	678.43	601.58	298.18	886.52	770.73	683.35	627.01	312.68
	S.D.	21.41	23.93	23.35	14.47	11.70	6.89	16.80	13.00	20.59	2.62
G_0	mL/g VS_{added}	558.63	510.36	497.10	443.59	244.39	626.82	552.26	490.69	459.60	250.19
	S.D.	22.39	18.93	16.28	11.43	8.46	6.72	11.50	9.89	14.15	3.39
First order model											
G_0	mL/g VS	635.80	537.83	511.02	455.99	239.79	691.33	593.75	515.13	480.58	236.15
	% difference	13.81	5.38	2.80	2.80	1.88	10.29	7.51	4.98	4.57	5.61
k	1/day	0.05	0.07	0.08	0.09	0.11	0.07	0.08	0.10	0.11	0.19
R^2	N/A	0.9800	0.9884	0.9829	0.9839	0.9788	0.9672	0.9667	0.9712	0.9702	0.9878
R^2 Adj	N/A	0.9743	0.9850	0.9780	0.9793	0.9727	0.9579	0.9572	0.9630	0.9617	0.9743
RMSE	N/A	31.18	21.42	25.23	22.02	12.59	47.43	41.17	33.33	31.89	8.54
AIC	N/A	74.51	67.00	70.27	67.55	56.38	82.90	80.07	75.84	74.96	48.62
Modified Gompertz model											
G_0	mL/g VS	496.11	461.48	453.62	414.34	213.21	623.80	547.80	485.23	454.63	218.07
	% difference	11.19	9.58	8.75	6.59	12.76	0.48	0.81	1.11	1.08	12.84
R_m	mL/g VS/day	54.35	46.07	50.31	41.25	31.95	48.64	52.50	51.99	48.84	42.74
λ	days	4.57	2.92	2.37	1.85	2.05	2.69	2.62	2.00	1.57	0.46
R^2	N/A	0.9446	0.9671	0.9752	0.9849	0.9578	0.9991	0.9937	0.9964	0.9966	0.9300
R^2 Adj	N/A	0.9168	0.9507	0.9629	0.9773	0.9367	0.9987	0.9905	0.9945	0.9949	0.8949
RMSE	N/A	48.60	33.10	27.84	19.32	17.11	7.40	17.80	12.59	9.93	20.04
AIC	N/A	87.67	79.99	76.53	69.23	66.79	50.03	67.59	57.66	55.91	69.95
Chen and Hashimoto model											
G_0	mL/g VS	857.81	696.30	640.27	567.35	290.60	903.03	753.02	629.74	582.87	269.43
	% difference	53.56	36.43	28.80	27.90	18.91	44.07	36.35	28.34	26.82	7.69
k_{CH}	N/A	22.40	22.25	18.39	18.31	19.40	17.04	17.12	16.98	16.13	121.56
μ_m	1/day	0.97	1.43	1.60	1.71	2.33	1.08	1.40	1.93	1.99	30.48
R^2	N/A	0.9768	0.9834	0.9748	0.9738	0.9737	0.9541	0.9484	0.9478	0.9455	0.9980
R^2 Adj	N/A	0.9652	0.9751	0.9622	0.9607	0.9605	0.9312	0.9226	0.9218	0.9182	0.9652
RMSE	N/A	30.10	22.79	27.69	25.30	13.36	50.59	47.07	41.42	39.72	3.37
AIC	N/A	78.09	72.53	76.42	74.62	61.85	88.48	87.03	84.47	83.64	34.28
Transfer model											
G_0	mL/g VS	524.58	504.39	496.05	457.32	231.16	687.01	588.67	522.93	492.33	239.19
	% difference	6.09	1.17	0.21	3.10	5.41	9.60	6.59	6.57	7.12	4.39
R_m	mL/g VS/day	54.35	46.07	50.31	41.25	31.95	48.64	52.50	51.99	48.84	42.74
λ	days	1.76	1.05	0.79	0.45	0.64	0.87	0.76	0.31	0.17	0.00
R^2	N/A	0.9603	0.9838	0.9838	0.9845	0.9753	0.9700	0.9695	0.9685	0.9627	0.9880
R^2 Adj	N/A	0.9366	0.9758	0.9757	0.9768	0.9629	0.9550	0.9542	0.9528	0.9440	0.9820
RMSE	N/A	45.79	23.01	22.27	19.54	13.05	41.02	36.23	32.45	33.31	9.08
AIC	N/A	79.64	72.72	72.07	69.45	61.38	84.28	81.80	79.60	80.12	54.12
Cone model											
G_0	mL/g VS	595.89	536.87	504.12	450.20	241.42	649.31	573.50	502.29	468.20	262.29
	% difference	6.67	5.19	1.41	1.49	1.21	3.59	3.85	2.36	1.87	4.84
k	1/day	0.08	0.10	0.13	0.13	0.16	0.11	0.12	0.15	0.16	0.26
n	N/A	1.86	1.71	1.87	1.91	1.73	2.40	2.34	2.35	2.40	1.10
R^2	N/A	0.9942	0.9974	0.9958	0.9971	0.9899	0.9981	0.9926	0.9944	0.9945	0.9985
R^2 Adj	N/A	0.9912	0.9962	0.9937	0.9957	0.9849	0.9971	0.9890	0.9916	0.9917	0.9978
RMSE	N/A	15.13	8.98	11.35	8.41	8.32	11.27	18.56	14.45	13.27	2.92
AIC	N/A	64.34	53.91	58.59	52.59	52.38	58.45	68.42	63.42	61.70	31.44
Superimposed model											
G_{01}	mL/g VS	0.00	370.24	331.81	286.17	150.06	6.92	167.66	275.48	271.16	153.58
G_{02}	mL/g VS	542.09	187.19	189.99	171.43	101.44	619.69	384.06	216.03	189.12	94.29
	% difference	2.96	9.22	4.97	3.16	2.91	0.03	0.10	0.17	0.15	0.92
R_m	mL/g VS_{added}/day	28.91	25.95	38.60	32.12	30.47	45.77	37.10	37.63	40.35	38.94
k	1/day	1.45	0.04	0.06	0.06	0.06	49.97	0.18	0.13	0.13	0.10
λ	days	1.95	3.10	3.30	3.19	2.72	2.57	4.30	4.58	4.73	0.42
R^2	N/A	0.9886	0.9988	0.9995	0.9994	0.9994	0.9997	0.9977	0.9987	0.9986	0.9993
R^2 Adj	N/A	0.9744	0.9972	0.9990	0.9986	0.9986	0.9992	0.9949	0.9971	0.9968	0.9744
RMSE	N/A	21.55	6.26	3.79	3.89	2.16	4.51	9.92	6.58	6.50	1.98
AIC	N/A	86.41	61.69	51.65	52.14	40.37	55.14	70.89	62.67	62.44	38.64
Modified Gompertz with second order equation model											
G_{01}	mL/g VS	0.00	505.77	412.77	323.13	202.88	49.09	108.90	197.87	189.55	243.19
G_{02}	mL/g VS	542.09	247.13	243.42	225.77	95.61	584.37	451.92	312.34	289.00	27.24
	% difference	2.96	47.52	32.00	23.74	22.14	1.06	1.55	3.98	4.12	8.09
R_m	mL/g VS/day	28.91	28.16	39.24	32.91	28.64	44.05	41.82	42.94	43.24	66.15
k	days	0.00	44.37	29.38	22.22	18.15	6.39	3.11	4.77	4.82	4.74
λ	days	1.95	2.49	2.78	2.61	2.87	2.82	3.48	3.73	3.61	1.48
R^2	N/A	0.9886	0.9983	0.9989	0.9988	0.9996	0.9996	0.9974	0.9984	0.9981	0.9997
R^2 Adj	N/A	0.9744	0.9962	0.9975	0.9974	0.9990	0.9992	0.9942	0.9965	0.9957	0.9744
RMSE	N/A	21.55	7.28	5.85	5.35	1.72	4.47	10.52	7.16	7.47	1.33
AIC	N/A	86.41	64.69	60.34	58.54	35.83	54.94	72.07	64.37	65.20	30.65
Two-phase exponential model											

(*continued on next page*)

Table 3 (*continued*)

FW:DSS Parameter	Unit	ADCM					ADWAS				
		1:0	4:1	2:1	4:3	0:1	1:0	4:1	2:1	4:3	0:1
G_{01}	mL/g VS	217.76	153.76	142.31	127.03	119.72	313.41	154.60	158.17	134.37	99.70
G_{02}	mL/g VS	418.04	384.07	368.71	328.96	120.07	313.41	439.14	356.95	346.20	154.46
	% difference	13.81	5.38	2.80	2.80	1.88	0.00	7.51	4.98	4.56	1.59
k_1	1/day	0.047	0.066	0.083	0.088	0.108	0.078	0.081	0.105	0.111	0.059
k_2	1/day	0.047	0.066	0.083	0.088	0.108	0.078	0.081	0.105	0.111	0.333
R^2	N/A	0.9800	0.9884	0.9829	0.9839	0.9788	0.9711	0.9667	0.9712	0.9702	0.9986
R^2 Adj	N/A	0.9640	0.9790	0.9692	0.9710	0.9618	0.9481	0.9401	0.9482	0.9463	0.9640
RMSE	N/A	31.18	21.42	25.23	22.02	12.59	52.32	41.17	33.33	31.89	2.81
AIC	N/A	84.80	77.28	80.56	77.84	66.67	95.15	90.36	86.13	85.25	36.64
Multi-stage model											
A_S	mL/g VS	0.00	0.00	0.00	0.00	0.00	0.00	0.00	0.03	0.00	31.03
A_I	mL/g VS	0.00	9.26	3.41	0.00	4.06	0.00	0.00	0.00	0.00	193.61
A_{IS}	mL/g VS	564.47	499.15	484.30	436.88	228.69	639.69	562.05	493.94	461.50	16.21
	% difference	1.05	0.38	1.89	1.51	4.76	2.05	1.77	0.67	0.41	3.73
k_1	1/day	0.29	0.52	0.53	0.52	0.89	0.18	0.21	0.26	0.27	1.00
k_2	1/day	0.09	0.09	0.12	0.13	0.14	0.18	0.21	0.26	0.27	0.16
R^2	N/A	0.9938	0.9966	0.9937	0.9952	0.9855	0.9968	0.9938	0.9948	0.9943	0.9928
R^2 Adj	N/A	0.9860	0.9923	0.9857	0.9892	0.9674	0.9928	0.9860	0.9883	0.9873	0.9837
RMSE	N/A	15.69	10.38	14.08	10.94	9.96	13.80	16.38	13.10	12.82	6.63
AIC	N/A	80.06	71.80	77.90	72.84	70.98	77.50	80.92	76.45	76.01	62.84

The table represents summary of kinetic analyses at different mixing ratios (1:0. 4:1, 2:1, 4:3, and 0:1) and different inocula for mono-digestion and co-digestion of food waste and dewatered sewage sludge. ADCM: Anaerobically digested cattle manure; ADWAS: Anaerobically digested waste activated sludge; B_0: Maximum specific biogas yield of substrates; G_0, G_{01}, G_{02}, A_S, A_I, A_{IS}: Maximum specific methane yield of substrates at respective phase and stage; R_m: Maximum methane production rate; λ: Lag phase, t: Time (days); k_{CH}: Chen and Hashimoto constant; μ_m: Maximum specific growth rate of microorganisms; k (1/day): Methane production rate constant (first order disintegration rate constant); k: Cone kinetic constant; n: Shape factor; k (days): First-stage half saturation time; k_1 and k_2: kinetic rate constants; R^2: Coefficient of determination; R^2 Adj: Adjusted R^2; RMSE: Root mean square error; AIC: Akaike's information criterion, N/A: Not applicable.

ADWAS (0.07–0.19) than ADCM (0.05–0.11), which also followed the same trend in the cone model. The higher kinetic constant indicates higher hydrolytic activity in ADWAS, corresponding to higher SMYs for ADWAS. Higher FW ratio in co-feedstocks resulted in lower first order kinetic constant even though FW has higher biodegradability than DSS. Slightly slower reaction rates might be due to the higher compatibility of DSS to ADWAS. Lower kinetic constant in higher FW content samples might be due to initial acidification. Low ISR of 1.0 adopted in this study could have potentially inhibited methanogenesis.

Based on the modified Gompertz model, higher fraction of FW resulted in an extended lag phase. Pan et al. (2019) also reported similar observation with FW content over 50%, which might be due to VFA accumulation. Hence, during co-digestion of FW and DSS, a higher share of FW could reduce the hydrolysis rate and prolong the lag phase.

From the kinetic analysis, it was evident that different kinetic models favored different systems (mono- or co-digestion) based on the types of feedstock. For CP:CM, cone model favored mono-digestion, while modified Gompertz with second order equation depicted the best-fit for co-digestion. Besides, for the same feedstock combination, error functions also resulted in different best-fitting models (modified Gompertz with second order equation based on R^2 Adj and RMSE, and cone for AIC). However, for FW:DSS, superimposed model was the best-fit for both mono- and co-digestion studies. It is important to note that both superimposed and modified Gompertz with second order equation models are derived from modified Gompertz and are thus similar in terms of model-fitting with BMP data.

4. Conclusion

Mono-digestion of CP and FW showed improved biodegradability, and significantly enhanced methane yield compared to their respective co-digestion with CM and DSS. ADWAS proved to be a better inoculum for the degradation of all the feedstocks tested. Furthermore, all the mixing ratios showed no substantial synergistic or antagonistic effect. In terms of kinetic model evaluation, it was evident that feedstock type has a major influence on the selection of best-fit model. It was also observed that co-digestion models can also fit better with mono-digestion results.

CRediT authorship contribution statement

Renisha Karki: Investigation, Visualization, Formal analysis, Writing – original draft. **Wachiranon Chuenchart:** Investigation, Visualization, Formal analysis, Writing – original draft. **K.C. Surendra:** Conceptualization, Supervision, Writing - review & editing. **Shihwu Sung:** Writing - review & editing. **Lutgarde Raskin:** Writing - review & editing. **Samir Kumar Khanal:** Supervision, Conceptualization, Writing - review & editing.

Declaration of Competing Interest

The authors declare that they have no known competing financial interests or personal relationships that could have appeared to influence the work reported in this paper.

Acknowledgments

The authors would like to acknowledge funding support from a Supplemental Grant through the United States Department of Agriculture (USDA), College of Tropical Agriculture and Human Resources, University of Hawai'i at Mānoa.

Appendix A. Supplementary data

Supplementary data to this article can be found online at https://doi.org/10.1016/j.biortech.2021.126063.

References

Astals, S., Koch, K., Weinrich, S., Hafner, S.D., Tait, S., Peces, M., 2020. Impact of storage conditions on the methanogenic activity of anaerobic digestion inocula. Water (Switzerland) 12, 1–12.

Bedoić, R., Špehar, A., Puljko, J., Čuček, L., Ćosić, B., Pukšec, T., Duić, N., 2020. Opportunities and challenges: Experimental and kinetic analysis of anaerobic co-digestion of food waste and rendering industry streams for biogas production. Renew. Sustain. Energy Rev. 130, 109951.

Chuenchart, W., Logan, M., Leelayouthayotin, C., Visvanathan, C., 2020. Enhancement of food waste thermophilic anaerobic digestion through synergistic effect with

chicken manure. Biomass Bioenergy 136, 105541. https://doi.org/10.1016/j.biombioe.2020.105541.
Corro, G., Pal, U., Cebada, S., 2014. Enhanced biogas production from coffee pulp through deligninocellulosic photocatalytic pretreatment. Energy Sci. Eng. 2 (4), 177–187.
Chala, B., Oechsner, H., Müller, J., 2019. Introducing temperature as variable parameter into kinetic models for anaerobic fermentation of coffee husk, pulp and mucilage. Appl. Sci. 9.
Dennehy, C., Lawlor, P.G., McCabe, M.S., Cormican, P., Sheahan, J., Jiang, Y., Zhan, X., Gardiner, G.E., 2018. Anaerobic co-digestion of pig manure and food waste; effects on digestate biosafety, dewaterability, and microbial community dynamics. Waste Manag. 71, 532–541.
Ebner, J.H., Labatut, R.A., Lodge, J.S., Williamson, A.A., Trabold, T.A., 2016. Anaerobic co-digestion of commercial food waste and dairy manure: characterizing biochemical parameters and synergistic effects. Waste Manag. 52, 286–294.
Elalami, D., Carrere, H., Monlau, F., Abdelouahdi, K., Oukarroum, A., Barakat, A., 2019. Pretreatment and co-digestion of wastewater sludge for biogas production: Recent research advances and trends. Renewable Sustainable Energy Rev. 114, 109287.
Gu, J., Liu, R., Cheng, Y.i., Stanisavljevic, N., Li, L., Djatkov, D., Peng, X., Wang, X., 2020. Anaerobic co-digestion of food waste and sewage sludge under mesophilic and thermophilic conditions: focusing on synergistic effects on methane production. Bioresour. Technol. 301, 122765.
Holliger, C., Alves, M., Andrade, D., Angelidaki, I., Astals, S., Baier, U., Bougrier, C., Buffière, P., Carballa, M., De Wilde, V., Ebertseder, F., Fernández, B., Ficara, E., Fotidis, I., Frigon, J.C., De Laclos, H.F., Ghasimi, D.S.M., Hack, G., Hartel, M., Heerenklage, J., Horvath, I.S., Jenicek, P., Koch, K., Krautwald, J., Lizasoain, J., Liu, J., Mosberger, L., Nistor, M., Oechsner, H., Oliveira, J.V., Paterson, M., Pauss, A., Pommier, S., Porqueddu, I., Raposo, F., Ribeiro, T., Pfund, F.R., Strömberg, S., Torrijos, M., Van Eekert, M., Van Lier, J., Wedwitschka, H., Wierinck, I., 2016. Towards a standardization of biomethane potential tests. Water Sci. Technol. 74, 2515–2522.
Jones, C.A., Coker, C., Kirk, K., Reynolds, L., 2019. Food waste co-digestion at water resource recovery facilities. Business Case Analysis.
Kafle, G.K., Chen, L., 2016. Comparison on batch anaerobic digestion of five different livestock manures and prediction of biochemical methane potential (BMP) using different statistical models. Waste Manag. 48, 492–502.
Karki, R., Chuenchart, W., Surendra, K.C., Shrestha, S., Raskin, L., Sung, S., Hashimoto, A., Kumar Khanal, S., 2021. Anaerobic co-digestion: current status and perspectives. Bioresour. Technol. 330, 125001.
Kaza, S., Lisa, Y., Perinaz, B., Frank, W., 2018. What a waste 2.0: a global snapshot of solid waste management to 2050. urban development series. World Bank, Washington, DC.
Koch, K., Hafner, S.D., Weinrich, S., Astals, S., Holliger, C., 2020. Power and limitations of biochemical methane potential (BMP) tests. Front. Energy Res. 8, 1–4.
Koch, K., Helmreich, B., Drewes, J.E., 2015. Co-digestion of food waste in municipal wastewater treatment plants: effect of different mixtures on methane yield and hydrolysis rate constant. Appl. Energy 137, 250–255.
Lima, D.R.S., Adarme, O.F.H., Baêta, B.E.L., Gurgel, L.V.A., de Aquino, S.F., 2018. Influence of different thermal pretreatments and inoculum selection on the biomethanation of sugarcane bagasse by solid-state anaerobic digestion: a kinetic analysis. Ind. Crops Prod. 111, 684–693.
Liu, C., Li, H., Zhang, Y., Liu, C., 2016. Improve biogas production from low-organic-content sludge through high-solids anaerobic co-digestion with food waste. Bioresour. Technol. 219, 252–260.
Londoño-Hernandez, L., Ruiz, H.A., Cristina Ramírez, T., Ascacio, J.A., Rodríguez-Herrera, R., Aguilar, C.N., 2020. Fungal detoxification of coffee pulp by solid-state fermentation. Biocatal. Agric. Biotechnol. 23, 101467.
Ma, G., Ndegwa, P., Harrison, J.H., Chen, Y., 2020. Methane yields during anaerobic co-digestion of animal manure with other feedstocks: a meta-analysis. Sci. Total Environ. 728, 138224.
Mao, C., Xi, J., Feng, Y., Wang, X., Ren, G., 2019. Biogas production and synergistic correlations of systematic parameters during batch anaerobic digestion of corn straw. Renew. Energy 132, 1271–1279.
Mao, C., Zhang, T., Wang, X., Feng, Y., Ren, G., Yang, G., 2017. Process performance and methane production optimizing of anaerobic co-digestion of swine manure and corn straw. Sci. Rep. 7, 1–9.
Masih-Das, J., Tao, W., 2018. Anaerobic co-digestion of foodwaste with liquid dairy manure or manure digestate: co-substrate limitation and inhibition. J. Environ. Manage. 223, 917–924.
Mata-Alvarez, J., Dosta, J., Romero-Güiza, M.S., Fonoll, X., Peces, M., Astals, S., 2014. A critical review on anaerobic co-digestion achievements between 2010 and 2013. Renew. Sustain. Energy Rev. 36, 412–427.
Mostafa Imeni, S., Pelaz, L., Corchado-Lopo, C., Maria Busquets, A., Ponsá, S., Colón, J., 2019. Techno-economic assessment of anaerobic co-digestion of livestock manure and cheese whey (Cow, Goat & Sheep) at small to medium dairy farms. Bioresour. Technol. 291, 121872.
Pan, Y., Zhi, Z., Zhen, G., Lu, X., Bakonyi, P., Li, Y.-Y., Zhao, Y., Rajesh Banu, J., 2019. Synergistic effect and biodegradation kinetics of sewage sludge and food waste mesophilic anaerobic co-digestion and the underlying stimulation mechanisms. Fuel 253, 40–49.
Panigrahi, Sagarika, Sharma, Hari Bhakta, Dubey, Brajesh K., 2020. Anaerobic co-digestion of food waste with pretreated yard waste: A comparative study of methane production, kinetic modeling and energy balance. J. Cleaner Prod. 243, 118480.
Paranhos, A.G.d.O., Adarme, O.F.H., Barreto, G.F., Silva, S.d.Q., Aquino, S.F.d., 2020. Methane production by co-digestion of poultry manure and lignocellulosic biomass: kinetic and energy assessment. Bioresour. Technol. 300, 122588.
Rojas-Sossa, J.P., Murillo-Roos, M., Uribe, L., Uribe-Lorio, L., Marsh, T., Larsen, N., Chen, R., Miranda, A., Solís, K., Rodriguez, W., Kirk, D., Liao, W., 2017. Effects of coffee processing residues on anaerobic microorganisms and corresponding digestion performance. Bioresour. Technol. 245, 714–723.
Selvankumar, T., Sudhakar, C., Govindaraju, M., Selvam, K., Aroulmoji, V., Sivakumar, N., Govarthanan, M., 2017. Process optimization of biogas energy production from cow dung with alkali pre-treated coffee pulp. 3 Biotech 7.
Tsapekos, P., Kougias, P.G., Kuthiala, S., Angelidaki, I., 2018. Co-digestion and model simulations of source separated municipal organic waste with cattle manure under batch and continuously stirred tank reactors. Energy Convers. Manag. 159, 1–6.
Wang, Z., Jiang, Y., Wang, S., Zhang, Y., Hu, Y., Hu, Z., 2020b. Impact of total solids content on anaerobic co-digestion of pig manure and food waste : Insights into shifting of the methanogenic pathway. Waste Manag. 114, 96–106.
Zahan, Z., Othman, M.Z., Muster, T.H., 2018. Anaerobic digestion/co-digestion kinetic potentials of different agro-industrial wastes: a comparative batch study for C/N optimisation. Waste Manag. 71, 663–674.
Zhen, G., Lu, X., Kobayashi, T., Kumar, G., Xu, K., 2016. Anaerobic co-digestion on improving methane production from mixed microalgae (Scenedesmus sp., Chlorella sp.) and food waste: kinetic modeling and synergistic impact evaluation. Chem. Eng. J. 299, 332–341.

Further reading

Wang, Y., Zhang, J., Li, Y., Jia, S., Song, Y., Sun, Y., Zheng, Z., Yu, J., Cui, Z., Han, Y., Hao, J., Li, G., 2020a. Methane production from the co-digestion of pig manure and corn stover with the addition of cucumber residue: Role of the total solids content and feedstock-to-inoculum ratio. Bioresour. Technol. 306, 123172. https://doi.org/10.1016/j.biortech.2020.123172.